A Search for CO Emission in High Redshift Powerful Radio Galaxies

A. S. Evans[1] and D. B. Sanders

Institute for Astronomy, 2680 Woodlawn Drive, Honolulu, HI 96822

J. M. Mazzarella

IPAC, MS 100-22, California Institute of Technology, Jet Propulsion laboratory, Pasadena, CA 91125

P. M. Solomon

Astronomy Program, State University of New York, Stony Brook, NY 11794

C. Kramer

Institut de Radio Astronomic Millimetrima, 18012 Granada, Spain

and

S. J. E. Radford

National Radio Astronomy Observatory[2], Tucson, AZ 85721

Received _____, accepted _____

Ap.J.

[1] Guest Observer at the James Clerk Maxwell Telescope, which is operated by the Royal Observatory Edinburgh on behalf of the United Kingdom Science and Engineering Research Council (SERC), the Netherlands Organization for the Advancement of Pure Research (ZWO), and the Canadian National Research Council (NRC).

[2]The NRAO is operated by Associated Universities, Inc., under cooperative agreement with the National Science Foundation

ABSTRACT

Upper limits for the molecular gas mass of 11 high redshift ($1 < z < 4$) powerful radio galaxies (HzPRGs) are presented. These observations include some of the most sensitive extragalactic CO observations to date. The four best studied radio galaxies (3C 368, 4C 23.56, B2 0902+34, and 4C 41.17) have less than one-third the CO luminosity of the hyperluminous infrared galaxy *IRAS* F10214+4724, and, assuming a Galactic CO-to-H_2 ratio, they have molecular gas masses comparable to or less than the most gas-rich, ultraluminous infrared galaxies (ULIGs) in the local ($z \leq 0.3$) Universe (i.e. $M(H_2) < 2\text{---}3 \times 10^{10} h^{-2} M_\odot$; $H_0 = 100h$ km s^{-1} Mpc^{-1} and $q_0 = 0.5$). Spectral energy distributions of 8 HzPRGs show them to have UV-to-optical luminosities ranging from a factor of ~ 0.1 to 1.0 that of the the UV-to-optical luminosity of F1 021 4+-4724. Recent submillimeter observations of 3 HzPRGs suggest that one source, 4C 41.17, may have an intense submillimeter-to-far-infrared excess. However, coadded *IRAS* observations suggest that HzPRGs as a class are not hyperluminous at far-infrared wavelengths. We also consider how the possibility that F 10214+4724 is a gravitationally lensed galaxies affects our interpretation of the data, as well as what it may mean for gas-rich galaxies in genera].

Subject headings: early universe - radio: galaxies - galaxies: interstellar matter - galaxies

1. INTRODUCTION

Studies of low-redshift ($z \leq 0.3$) powerful radio galaxies (LzPRGs; $P_{408\mathrm{MHz}} \gtrsim 1024\ h^{-2}$ Watts Hz-l) have provided evidence that many may be rich in gas and dust. Deep optical imaging of a complete sample of LzPRGs led Heckman et al. (1986) to conclude that a substantial fraction probably arise from the collision /merger of galaxy pairs, at least one member of which is a disk galaxy. Golombek, Miley, & Neugebauer (1988) found that a significant fraction of LzPRGs are luminous far-infrared sources. From a study of a complete sample of 'warm' ULIGs, Sanders et al. (1988) suggested that ULIGs, quasars, and powerful radio gal axies may represent an evolutionary sequence in the merger of gas-rich spiral galaxies. CO($1 \rightarrow 0$) emission and HI absorption (Mirabel 1989, Mirabel, Sanders, & Kazès 1989) confirmed the existence of dense concentrations of both atomic and molecular gas in the nuclei of at least some LzPRGs, while a more extensive survey of CO emission from LzPRGs by Mazzarella et al. (1993) indicated that rich supplies of molecular gas may indeed be ubiquitous in powerful radio-selected galaxies detected by *IRAS*.

Powerful radio galaxies at $z \sim 1$ are also observed to have the multicomponent structures and/or nearby companions commonly associated wit h merging galaxies (e.g., Spinrad & Djorgovski 1984a, b; Lilly& Longair 1984; Djorgovski et al. 1987). More recent observations have extended detections of powerful radio galaxies out to redshifts $z \sim 4$ (scc the review by McCarthy 1993). While the nature of these high redshift powerful radio galaxies (HzPRGs; $P_{408\mathrm{MHz}} \gtrsim 1027\ h^{-2}$ watts Hz^{-1}) is still controversial (e.g., McCarthy et al. 1987, Chambers, Miley, & van Breugel 1987, 1990; Rigler et al. 1992; Dunlop & Peacock 1993; Eales & Rawlings 1993), it is possible that these objects, observed out to an epoch when the Universe was 10–20% of its present age, arc more extreme examples of the gas-rich LzPRGs that have been dctcctcd in CO. The most molecular gas-rich LzPRG currently known is 4C 12.50 (= PKS1345+12; $z = 0.12$) with $M(H_2) \sim 2.5 \times 10^{10} h^{-2}\ \mathrm{M}_\odot$ (Mirabel et al. 1989).

Recently, the possibility of detecting CO emission at z >2 has been demonstrated at several single-dish millimeterwave telescopes by the measurement of several CO rotational transitions in the hyperluminous infrared galaxy *IRAS* F1 0214+4724 at z = 2.286 (Brown & Vanden Bout 1991, 1992; Solomon, Dowries, & Radford 1992a; Tsuboi & Nakai 1992). Although these lines arc the weakest extragalactic CO emission lines yet detected, their strengths have been verified by repeated long integrations and by observations of the same transitions with different telescopes. The observed CO lines ratios are consistent with emission from warm ($T_{\rm kin} \simeq 30 - 60$ K), optically thick molecular clouds, similar to the molecular gas in the cores of nearby luminous infrared galaxies. The apparent CO luminosity of F10214 implies a molecular gas mass, $M(\mathrm{H_2}) \sim 10^{11} h^{-2}\,\mathrm{M_\odot}$ (Solomon et al. 1992a). This is only ~ 4 times more molecular gas than that derived for the most gas-rich LzPRGs (e.g. 4C 12.50). It therefore seems reasonable that H zPRGs may have more than a factor of 4 more molecular gas than LzPRGs, and thus we might have a reasonable chance of detecting CO emission from HzPRGs with the current generation of millimeterwave telescopes.

In this paper, we extend CO observations of powerful radio galaxies to redshifts 1-4 by observing 11 HzPRGs with well determined redshifts. in §2, we discuss how these HzPRGs were selected. Observing procedures are presented in §3. in §4, the data reduction methods arc summarized, and a comparison of spectra for galaxies observed with more than one telescope is presented. Upper limits are calculated for the C() luminosity and H_2 gas mass for the 11 HzPRGs. The discussion in §5 compares these data and the spectral energy distributions of HzPRGs with previous data for F1021 4+4724, lower redshift ULIGs, and IRAS selected powerful radio galaxies. Section 6 summarizes our results.

2. SAMPLE SELECTION

High redshift radio galaxies spanning a range $1 < z < 4$ were initially selected for observation based on the accuracy of their published redshifts and the availability of CO lines redshifted to frequencies accessible by millimeter-wave telescopes. Positions of additional unpublished HzPRGs were obtained (K. Chambers, private communication) and their redshifts confirmed by infrared spectroscopy when possible (Evans & Sanders 1995). Over the course of the survey, 15 radio galaxies were observed, and adequate integration times (i.e., longer than 9 hours with the NRAO 12m telescope or longer than 1 hour at the IRAM 30m telescope) were obtained for 11 HzPRGs. Five of these 11 HzPRGs have been discussed extensively in the literature, and their properties are summarized briefly below:

3C 368 (z = 1.132) - one of the bluest radio galaxies known and the prototypical "(aligned" radio galaxy (Chambers, Miley, & Joyce 1988). For a nearly normal galaxy, a blue color is indicative of a young stellar population]). However, the presence of an AGN and radio jets prevent us from making such a straight-forward interpretation of colors in this case. Based on the multicomponent morphology of 3C 368 and the behavior of the ionized-gas velocity field, Djorgovski et al. (1987) proposed that 3C 368 is a dissipative merger.

3C 68.2 (z = 1.575) - a very red radio galaxy (e.g. Chambers & Charlot 1990). For a nearly normal galaxy, a red color is indicative of an old stellar population. However, given the AGN nature of 3C 68.2, the contribution of non-stellar emission to the broad-band colors is uncertain.

MG 1019+054 (z = 2.765) - one of the few known HzPRGs with depleted Lyα emission. Such a depiction may be due to scattering of Lyα photons by dust (Dey, Spinrad, & Dickinson 1995).

B2 0902+34 (z = 3.397) - the first radio galaxy discovered at a redshift greater than 3 (Lilly 1988). Based on the flatness of the SED (F_ν vs. λ) at V and I band, Lilly (1988)

concluded that the galaxy has a young stellar component. The apparent rise in the SED towards K band, which Lilly (1 988) suggested may be due to either an old stellar population or strong [0 III] 4959 and 5007 emission lines, was confirmed by Eisenhardt & Dickinson (1992) and Eales & Rawlings (1 993) to be due to strong [0 III] emission lines. Indeed, the emission lines appear to be responsible for $\sim$90% of the K band flux. Of all of the radio galaxies observed by Eales & Rawlings (1993) in their K band spectroscopic survey, B2 0902+34 is the best candidate for a galaxy with a zero-age stellar population. Such a conclusion, however, relies on the assumption that the continuum emission is primarily from stars and not from sc.attered/reprocessed/beamed nuclear light. B2 0902+34 is also noteworthy for being a reported source of H I absorption (z = 3.3968: Uson, Bagri, & Cornwell 1 991; Briggs, Sorar, & Taramopoulos 1993).

4C *41.17* *(z = 3.797)* - the highest redshift galaxy known at the time we began our survey. Dunlop ct al. (1 994) and Chini & Krügel (1994) have detected emission from dust in 4C 41.17 by submillimeter observations (we will discuss this further in §5.1).

The six other HzPRGs observed in CO and discussed in this paper arc TX 0200+015, TX 0828+193, 4C 26.38, 4C 23.56, MG 2141 +19, and 4C 28.58, most of which arc steep spectrum radio sources (see McCarthy 1993 for a review of search techniques for HzPRGs).

3. 013 SERVATIONS

Table 1 summarizes basic information and a journal of observations for the radio galaxies discussed in this paper. Observations with each of the telescopes used in this survey arc discussed separately below.

3.1. NRAO 12m Telescope

observations with the NRA() 12m telescope were obtained during six separate observing periods between 1992 December and 1995 January. With the exception of the last observing period, all of the observing sessions were marked by a high percentage of exceptionally good weather. All observations were obtained using a nutating subreflector with a chop rate of ~1.25 Hz. Data were stored as either five or six minute scans, and a chopper wheel calibration was typically performed after every other scan. Pointing was monitored every few hours by observations of the planets and was estimated to be accurate to ±3 arcseconds.

Data were obtained with the dual polarization] 3mm SIS receiver and two 512x2 MHz channel filterbanks, onc for each polarization. l'here were problems with our initial observations that forced us to eventually discard half of the data from 1992 December, and to revise our method of taking data for subsequent observing runs. Instabilities in one of the two receiver polarizations occasionally produced low level noise spikes that, if not caught and eliminated from the data stack, would, after smoothing, mimic narrow (~ 50- 100 krn s^{-1}) lines. Even though the channel blocks that were thought to be affected were eventually eliminated, we chose to throw out all of the 1992 Deçember data obtained with that polarization. We also decided to abandon our original attempt to double the velocity coverage of our observations by obtaining an equal amount of integration time for each source at three frequency settings, ν_0 and $\nu_0 \pm \Delta\nu$ (where Au corresponded to a velocity offset of 500 km s^{-1}). The increased total velocity coverage (~2500 km s^{-1}) had been designed to allow for uncertainties (typically 0.1 - 0.2%) in the reported redshifts for our sources. However, observations of a blank sky position at a fixed frequency revealed that, although the theoretical channel-to-channc] rms was achieved in each filterbank for the longest integrations, wc could not assume that the mean level was zero. Comparison of coaddcd data representing observations taken during consecutive 6-8 hr transits revealed that small, apparently random dc offsets and tilts in the baseline were often present at a level of a fcw x 0.1 mK. Had relatively strong (> 1 mK) lines been present in any of our sources

this method should still have served to increase our likelihood of achieving a detection. No such lines were detected. Instead, the large velocity shifts often had the effect of producing rather broad, pill box-shaped, phantom line profiles, and we therefore decided to drop our attempt to obtain extended velocity coverage on each source.

Even given the above precautions, with careful baseline subtraction, integrations of up to 8 hours showed spurious spectral features in subsequent observing periods that typically disappeared with longer integrations. Such ghost features, when smoothed, mimicked ~150 km s^{-1} emission lines. These features are possibly due to receiver instabilities or low level systematics, as well as irregularities caused by the Sun. Although the Sun never shone directly on the dish, coadded scans of daytime observations were noisier than nighttime observations, even for comparable system temperatures.

In addition to the baseline analysis, the reliability of the 12m data was tested by observing several faint, relatively nearby ULIGs in 1994 May and 1994 October. Published spectra exist for all but one of these galaxies (Sanders, Scoville, & Soifer 1991). After a few hours of integration per source, the expected peak CO line temperatures (T_{mb} = 3-15 mK) and line profiles were achieved.

3.2. JCMT 15m Telescope

Observations were made with the JCMT 15m Telescope during three observing periods between 1993 October and 1994 September. To obtain the largest velocity coverage possible, the 1 mm SIS receiver (A2) was used together with the newly commissioned DAS in wide-band mode (750 MHz bandwidth). Because of excess noise near the edge of the passband, the usable bandwidth was only ~700 MHz, which corresponds to a total velocity coverage of ~900 km s^{-1} at 230 GHz.

The basic observing technique at the 15m Telescope was similar to that used at the 12m telescope. However, because the total velocity coverage at 1mm with the DAS in wide-band mode was still significantly less than the velocity coverage for observations at 3mm with the 12m Telescope, velocity offsets at the 15m Telescope were limited to $\lesssim 100$ km S^{-1}. To test our ability to measure moderately weak lines, we made a one hour integration on IRAS 10173+0828, an ULIG previously detected in CO(1→0) (Sanders et al. 1991). The CO(2→1) line width ($\Delta v_{FWHM} \sim 150$ km s^{-1}) and peak temperature ($T_{mb} \sim 14$ mK) agree well with the CO(1→0) profile under the reasonable assumption that the ratio of main beam brightness temperatures, CO(2→1)/(1→0), is ~1.0 (i.e. the gas temperature is $\gtrsim 30 - 50$ K, typical of the warm gas temperatures associated with ULIGs). However, our ability to detect much weaker broad lines (i.e. $\lesssim 2$ mK, and $\Delta v_{FWHM} \gtrsim 300$ km s^{-1}) is less clear. Despite careful precautions, long integrations with the DAS revealed that the baselines of the spectra were bowed, a condition that would make it impossible to distinguish between a broad CO line and baseline curvature (see Röttgering et al. 1995 for additional comments on baseline curvature in JCMT spectra).

3.3. IRAM 30m Telescope

Observations at the IRAM 30m Telescope were made during four observing periods between 1994 June and 1994 December. With the exception of the observations of 4C 41.17, TX 0200+015 and MG 1019+054, I RAM time was used to confirm tentative CO detections from the other two telescopes. Not only does the IRAM telescope have a larger aperture than the other two telescopes, but it has the unique ability to perform observations using the 3mm, 2mm, and 1 mm receivers simultaneously. Since the best detections of CO in high redshift galaxies have been confirmed by observations of several transitions, this multi-frequency ability is extremely helpful in overcoming the difficulty of searching for weak signals because

(i) compared with sequential observations of different lines, the necessary integration is 2 or 3 times less, and *(ii)* observing different frequencies simultaneously ensures the telescope pointing, among other effects, is the same for all the lines. During the first two observing periods, we tuned both the 3mm and 2mm receivers to redshifted CO lines for each source, using one 512 x 1 MHz filterbank for each receiver. One 512 MHz bandwidth autocorrelator per receiver also was used as a double check. In the last two observing periods, we also tuned the 1 mm receiver to a redshifted CO line for a given source, switching one of the autocorrelators over for 1 mm observations.

To test the reliability of our 30m Telescope data, we observed the CO(3 → 2) transition of F1 0214+4724 during the 1994 December observing period. The observations yielded the expected peak CO line temperature ($T_{mb} \sim 4$ mK) and line profile shape as previously reported by Solomon et al, (1992).

4. RESULTS

4.1. CO Spectra

Table 2 summarizes the CO line data for our radio galaxy observations. In the case of galaxies for which data was taken at several widely spaced velocity offsets, we present those data in separate spectral blocks. Separating the data in this manner avoids the creation of dc offset-induced ghost features (see §3.1) and provides data blocks with consistent signal-to-noise across each spectrum.

Figure 1 shows the spectra obtained with the 12m Telescope. For every source, individual scans were examined to check for sinusoids in the baselines and other irregularities. Most of the difficulties with irregularities were encountered in the 1993 June observing period, and though obvious bad scans were removed, low level systematics could still be present

in seemingly "normal" scans. For example, it was unclear if the line at -3oO km s^{-1} in the spectrum of 4C 28.58 was a real emission line, or an artifact due to such systematic. After bad scans were removed, the rest of the scans were averaged and linear baselines were subtracted. For sources observed with several small velocity offsets, on] y the overlapping regions of the scans were averaged. This, in part, accounts for the differences in velocity coverage from source to source in Figure 1 (The other factor affecti ng the velocit y coverage is the change in velocity coverage, Av, as a function of the observing frequency, ν; Av = $c\Delta\nu/\nu$, where $\Delta\nu$ = 512 MHz.). Finally, we smoothed the spectra to $\sim$ 50 km s^{-1}. The end result of our 12m data reduction was that two objects, 4C 28.58 and B2 0902+34, appeared to have tentative detections.

Figure 2 shows the JCMT 15m spectra of 4C 23.56 CO(7 ---i 6) data and 4C 28.58 CO(8 $\rightarrow$ 7) data smoothed to a velocity resolution <40 km s]. The scans were reduced in the same fashion as the 12m data, but, baseline curvature was impossible to remove. The spectrum of 4 C 28.58 clearly shows a sinusoidal baseline ripple. Observations of 4 C 23.56 showed a feature at O km s-' in the 1993 October observing period, but subsequent observations did not confirm the feature. The spectrum in Figure 3 is a coadd of all three observing periods, with the hint of the O km S–l '<feature" barely visible. The 4C 23.56 coadds from the individual observing periods all had bowed baselines.

Figures 2-5 show the IRAM 30m spectra of the remaining sources. As is clear in Figure 2, the tentative detection of CO emission in 4C 23.56 and 4C 28.58 were not confirmed. Figure 4 shows the CO(4 $\rightarrow$ 3), CO(5 $\rightarrow$ 4), and the CO(8 $\rightarrow$ 7) spectra of B2 0902+34. The spectra do not confirm a line in this source either, though the first 10 hours of integration of the CO(5 $\rightarrow$ 4) data showed a tentative feature at +200 km S^{-1}.

4.2. CO Luminosity Limits

Table 2 lists the root-mean-square temperatures, $T_{\rm rms}$, achieved with a velocity resolution, $\Delta v_{\rm res}$, for the 11 HzPRGs observed. To calculate the upper limit of the CO line intensity, $I_{\rm CO}$, we assume that the CO lines have a FWHM velocity, $\Delta v_{\rm FWHM} \sim 250$ km S–l, similar to CO lines seen in local ULIGs (e.g. Sanders et al. 1991), LzPRGs (Mozzarella et al. 1993), and in F1 0214+4724 (e.g. Solomon et al. 1992a), Using the observed $T_{\rm rms}$ and $\Delta v_{\rm res}$ from Table 2, our 3σ limit on $I_{\rm CO}$ is given by

$$I_{CO} < \frac{3T_{\rm rms}\Delta v_{\rm FWHM}}{\sqrt{\Delta v_{\rm FWHM}/\Delta v_{\rm res}}} \ [\rm K\ km\ s^{-1}].$$

Multiplying $I_{\rm CO}$ by the Kelvin-to-Jansky conversion for a point source[3] gives the corresponding limit for $S_{\rm CO}\Delta v$ [Jy km S-l].

The luminosity distance for a source at a given redshift, z, is,

$$D_{\rm L} = cH_0^{-1} q_0^{-2} \left\{ zq_0 + (q_0 - 1)\left(\sqrt{2q_0 z + 1} - 1\right) \right\} \qquad [\rm h^{-1}\ Mpc],$$

where q_0 is the deceleration parameter (= 0.5 for a critical density universe) and $H_0 = 100h$ (km $\rm s^{-1} Mpc^{-1}$). Given our estimated intensity upper limit, $S_{\rm CO}\Delta v$, we can calculate the CO luminosity of a source at redshift z,

$$L'_{\rm CO} = \left(\frac{c^2}{2k\nu_{\rm obs}^2}\right) S_{\rm CO}\Delta v D_{\rm L}^2 (1+z)^{-3},$$

where c is the speed of light, k is the Boltzmann constant, and $\nu_{\rm obs}$ is the observed frequency. In terms of useful units, $L'_{\rm CO}$ for the CO(J -i J – 1) rotational transition can be written as,

$$L'_{\rm CO} = 2.4 \times 10^3 \left(\frac{S_{\rm CO}\Delta v}{\rm Jy\ km\ s^{-1}}\right)\left(\frac{D_{\rm L}^2}{\rm Mpc^2}\right) J^{-2}(1+z)^{-3} \ [\rm K\ km\ s^{-1}\ pc^2],$$

where [K km $\rm s^{-1}$] can bc expressed simply as [$L_\odot$].

---

[3]References for beam efficiencies and flux calibrations: NRAO 12m (P. Jewell, private communication), JCMT 15m (Matthews 199'2), IRAM 30m (Guelin, Kramer, & Wild 1995)

Table 2 lists the L'_{CO} upper limits of for the 11 HzPRGs observed. We have assumed that CO rotational transitions up to CO(4 → 3) have approximately the same brightness temperature. This assumption is based on previously published multi-transition CO analyses of F1 0214+4724, and the fact that the cosmic microwave background at these redshifts Contributes strongly to populating the lower CO levels, $T_{CBM} = 2.7(1 + z)$ K (e.g. Solomon et al. 1992a; Solomon, Radford, & Dowries 1992b). A plot of L'_{CO} vs. redshift for the 11 HzPRGs, F1 0214+4724, the lensed quasar H1413+135, and several low-redshift IRAS galaxies is presented in Figure 6. In the cases of all but two of the 11 observed radio galaxies, upper limits less than the L'_{CO} of F1 0214+4724 were observed. For 3C 368, 4C 23.56, B2 0902+34, and 4C 41.17, upper limits less than one-third the L'_{CO} of F10214+4724 were reached. The upper limits on L'_{CO} for these four HzPRGs are similar to the values of L'_{CO} measured for the most gas-rich ULIGs in the local Universe (e.g. IRAS 14348-1447, 4C 12.50), but are still 2-3 times higher that the value of L'_{CO} observed for Arp 220.

4.3. H_2 Masses

The upper limits on H_2 masses implied by the observed limits on L'_{CO} can be determined by making the reasonable assumption that the CO emission is optically thick and thermalized, and originates in gravitationally bound molecular clouds. For molecular gas in gravitationally bound clouds, the ratio of the H_2 mass and the CO luminosity is given by $\alpha = M(H_2)/L'_{CO} \propto \sqrt{n(H_2)}/T_b\ M_\odot$ (K km s^{-1} pc^2)$^{-1}$, where $n(H_2)$ and T_b are the density and brightness temperature for the appropriate CO transition (e.g. Sanders & Scoville 1987; Solomon et al. 1992a). Multi-transition CO surveys of molecular clouds in the Milky Way (e.g. Sanders et al. 1993), and in nearby starburst galaxies (e.g. Güsten et al. 1993) have shown that hotter clouds tend to be denser such that the density and temperature dependencies tend to cancel each other. The variation in the value of α is less than a factor

of 2 for a wide range of gas kinetic temperature, gas densities, and CO abundance. We adopt a value of 4 $M_\odot$ (K km s^{-1} $pc^2)^{-1}$ for α, which is similar to the value determined for the bulk of the molecular gas in the disk of the Milky Way (cf. Scoville & Sanders 1987), as well as the value determined from a multi-transition CO analysis of F1 0214+4724 (Solomon et al. 1992a). Figure 6 shows that the upper limits for $M(H_2)$ in the 11 HzRGs range from 2 to 11 x 10^{10} h^{-2} $M_\odot$.

5. D1SCUSS1ON

Our non-detection of CO emission in all of the observed HzPRGs is somewhat surprising. In particular, the CO luminosities of the four HzPRGs with the most sensitive upper limits (3C 368, 4C 23.56, B2 0902+34, and 4C 41 .17) are less than that of the most gas-rich LzPRGs previously detected in CO (e.g. 4C 12.50); this despite the fact that HzPRGs have radio luminosities typically a factor of 10–1 000 larger than the radio luminosities of LzPRGs detected in CO. Wc believe that our reported upper limits $(3\sigma)_{011}$ L'_{CO} for HzPRGs are, if anything, conservative, and that it is unlikely that CO luminosities above these limits have escaped detection. The two most likely ways to 'hide' such emission, through extremely broad linewidths or emission that falls outside the observed spectrometer passband, seem to be ruled out in the current observations. In particular, the CO linewidths in the observed HzPRGs would have to be systematically larger (e.g. $\Delta v_{FWHM} > 750$ km s^{-1} than any extragalactic CO linewidth measured to date, and the CO line centroid would have to differ by more than $\sim$ 500 km s^{-1} from the redshifts determined from the narrow optical and near infrared emission lines. For low-redshift objects detected in C(), the centroid of the CO emission is always within a few hundred km s^{-1} of the red shift determined from the narrow emission lines, and wc feel confident that this is the case for the HzPRGs.

The bulk of the radio emission in HzPRGs originates in their powerful extended radio

lobes (i.e. FR 11 sources), and our CO observations suggest that the radio lobe emission is not directly related to the molecular gas content of these objects. A similar conclusion was reached by Mozzarella et al. (1993) from observations of LzPRGs. In particular, all of the CO detections of powerful radio galaxies to date are of either core dominated or FR I sources. A correlation between L'_{CO} and radio power was found to exist for sources with radio power, P_{408MHz}, less than $\sim 10^{25}$ watts Hz^{-1}, whereas the upper limits on L'_{CO} for stronger radio sources (FR I I) are actually consistent with no increase, or even a decrease in CO luminosity. For example, in the nearest FR II source, the classic powerful radio galaxy Cygnus A (z = 0.058), the upper limit on the CO luminosity is one-tenth that of the most gas-rich LzPRG, 4 C 12.50, despite the fact that the radio power of Cygnus A is $\sim$ 100 times larger than for 4C 12.50. However, Mozzarella et al. (1993) did find that the correlation between $L_{ir}(8-1000\mu m)/L_{CO}$ and $L_{ir}(8-1000\mu m)$, that has been observed for lower luminosity infrared galaxies, ULIGs, and infrared selected QSOs, also appears to hold for LzPRGs. This would suggest that a more meaningful way to compare our CO observations of HzPRGs with LzPRGs would be to compare the ratio L_{ir}/L_{CO} in these objects.

5.1. Spectral Energy Distributions for HzPRGs

Figure 7 presents SEDs for 8 HzPRGs, three of which were observed in CO. These 8 objects are among the HzPRGs for which the largest amount of published photometric data are currently available. Also shown for comparison are the SEDs for the 'hyperluminous' infrared galaxy F1 *0214+4724*, and the LzPRGs with the highest observed CO luminosity, 4C 12.50. These SEDs show the following: (1) There is no current evidence that any of the HzPRGs emit a substantial fraction of their bolometric luminosity at far-infrared/submillimeter wavelengths ($\sim$1 0–1000 μm), and in particular that these objects

contain substantial amounts of cool dust. Except for the detection of 4C 41.17 at 800μm and an upper limit for 6C 1232+39 at 800pm, submillimeter observations for the remaining objects are nonexistent. Until sensitive submillimeter observations can be obtained, it is impossible to tell whether the spectral index of the submillimeter emission from HzPRGs has a slope steep enough to be consistent with thermal emission from dust. Also, IRAS observations only resulted in upper limits, and thus are useless in determining the shape of the far-infrared emission. For four of the 8 HzPRGs the IRAS data can be used to at least rule out the possibility that these objects are as luminous as F1 0214. (2) In contrast to the far-infrared/submillimeter data, all of the HzPRGs have been detected at optical-to-UV wavelengths. The optical -to-UV spectra are d iverse, but they all appear to exceed the luminosity of local powerful radio galaxies (e.g. 4C 12.50). The strongest optical-to-UV source, 6C1232+39, has a spectrum nearly identical to IRAS F10214+4724. Eales et al. (1993) have suggested that the structural differences observed in ll)ulti-wavelength imaging of 6C 1232+39 are due to dust, consistent with the U V-to-optical slope of the galaxy. The presence of dust in radio galaxies may account for the dramatic decrease in luminosity toward smaller wavelengths seen in most SEDs of HzPRGs. H owever, the interpretation of emission at these wavelength is somewhat controversial (cf. McCarthy 1993); it is not clear what percentage of the broad-band measurements are due to emission line contamination, or what percentage of the luminosity is stellar or scattered/beamed/reprocessed nuclear light.

5.2. Is F 10214+4724 a Gravitationally Lensed Galaxy?

There is now increasing evidence that *IRAS* F] 0214+4724 is a gravitationally lensed galaxy (Elston et al. 1 994; Soifer et al. 1995; Trentham 1995; Graham & Liu 1995; Broadhurst & Lehr)995; Serjeant et al. 1995). If F102I 4+4724 is lensed, radiation from the galaxy would be achromatically amplified, causing an overestimation in such measured

quantities as the infrared and CO luminosity (and thus the H_2 mass). It is worth noting here that the only other confirmed detection of CO emission at z >2 is for the lensed quasar H1413+135 ('The Cloverleaf') at z = 2,556 (Barvainis et al. 1994). If the amplification factor for these two objects is larger than $\sim$ 4 and $\sim$ 8 respectively, then both of these objects have intrinsic CO luminosities less than the the most luminous CO sources observed locally (z < 0.3).

Our search for CO in HzPRGs was strongly motivated by the similarities of ULIGs and powerful radio galaxies at low redshift and the success of detecting CO emission from F10214+4724 at a z = 2.286. Since we used the CO luminosity of F10214+4724 as a calibration of what to expect for gas-rich galaxies at high redshi ft, convincing proof that F1 0214+4724 is a lensed galaxy would mean we have undertaken our survey of HzPRGs with the false expectation that sources with intrinsic CO luminosities as strong as the observed L_{CO} of F10214+4724 actually exist.

Two conclusions relevant to this survey can be made based on the assumption that F10214+4724 is a lens. First, F1 0214+4724 may be no different from ULIGs we see locally. Indeed, the amount of molecular gas measured in the most gas-rich, local galaxies may be the largest amount of H_2 gas that exists in galaxies at any epoch. Second, our lack of success in detecting CO gas in HzPRGs may mean the similarities between ULIGs and powerful radio galaxies observed at low-redshift (see §1) hold for galaxies at high redshift. Active galaxies at redshifts of 2 or 3 may be no different than those observed at z $\sim$ O. On the basis of radio power, redshift, and morphology, it can be argued that powerful HzPRGs are at an earlier evolutionary stage than local radio galaxies. 1 lowever, the space density of powerful radio galaxies is low enough that the probability of finding one locally is low, and the observed morph ologies may be affected by scat tered/beamed /reprocessed nuclear light and line emission contamination (McCarthy, Elston, & Eisenhardt 1992; Eisenhardt & Dickinson 1992; Eales & Rawlings 1993; Eales & Rawlings 1995).

5.3. Implications of the Current Limits on L_{CO} in HzPRGs

There are several possible explanations why the HzPRGs, which are believed to be the progenitors of giant elliptical galaxies, were not detected in CO: (1) The red shift at which most of the stars in present day galaxies formed may be greater than 4. Thus, if the central engine is fueled by the same material as the starburst, these HzPRGs may be at the end of the initial starburst/AGN phase, or the AGN activity may simply be the result of a recent merger event. (2) An amount of molecular gas equivalent to the stellar mass of a present day elliptical galaxy may be distributed among many smaller, star-forming galaxies that eventually merge to form present day galaxies. This is feasible given that merger rates must have been higher in the past. (3) The duration a galaxy can have in excess of, $2 - 3 \times 10^{10} h^{-2}$ $M_{\odot}$ of molecular gas may be very brief. Thus, the probability of observing a galaxy in such a gas-rich state is low. (4) The universe may not have closure density. If the density of the universe is less than closure density, the scale of the universe is larger. The effect is most dramatic at higher redshifts; the upper limit estimate of L'_{CO} (and thus H_2 mass) in 4C 41.17 may be up to a factor of 4 larger (i.e., the empty universe cosmology, $q_0 = 0$).

6. SUMMARY

In this paper, CO observations of 11 high redshift radio galaxies have been presented. Compiled published photometry of 8 of the best studied HzPRGs were also presented for comparison with *IRAS* F10214+4724. The following conclusions are drawn:

(1) For 9 out of the 11 HzPRGs observed, we achieved upper $M(H_2)$ mass limits less than the H_2 mass of the hyperluminous source F10214+4724 ($z = 2.286$). For the galaxies 3C 368, 4C 23.56, B2 0902+34, and 4C 41.17, upper $M(H_2)$ limits less than a third the gas mass of F10214+4724 and comparable to the gas mass of the most gas-rich, local galaxies

were achieved.

(2) Currently available UV-to-radio SEDs of HzPRGs show them to have UV-to-optical luminosities ranging from a factor of ~ 0.1 to 1.0 that of the UV-to-optical luminosity of F1 0214+4724. In the case of 4C 41.17, there is possible evidence for "excess" emission at $\sim$ 200pm (object restframe: Chini & Krügel 1994; Dunlop et al. 1994), consistent with thermal emission from dust. However, the *IRAS* non-detections of all known HzPRGs indicate that HzPRGs as a class are not hyperluminous at infrared wavelengths.

(3) Our survey was strongly motivated by the successful detection of CO emission in F 10214+4724 and the possibility that F 10214+4724 may be a radio-quiet analog of HzPRGs. The non-detections of CO emission in HzPRGs arc consistent with recent evidence that F 10214+4724 is a gravitationally lensed galaxy; if the lensing factor is > 4, the intrinsic L_{CO} of F 10214+4724 would bc undetectable by available submillimeter telescopes.

Our search for CO emission in HzPRGs would appear to have pushed current single dish millimeterwavc telescopes c1osc to their practical limits. Given the upper $M(H_2)$ limits of our 4 best studied radio galaxies and the integration times required to achieve such limits, follow-up observations may have to wait for the availability of much larger apertures or much more sensitive millimeterwavc telescope arrays.

Wc thank the staffs of the NRAO 12m telescope, the JCMT 15m telescope, and IRAM 30m telescope for their generous support during our observations. We thank I. F. Mirabel, J. Wink, and S. A. Ealcs for allowing their IRAM 30m data for 4C 41.17 to be published in our paper and K. C. Chambers for providing redshifts and coordinates for some of the 4C sources that were observed, We acknowledge assistance from J .R. Graham with the initial 4C 41.17 observations. A.S.E. also thanks D. Jewitt, N. Trentham, J. Goldader, and G. Djorgovski for useful discussions and assistance during the preparation of this paper. A .S.E.

and).13.S. were supported in part by NASA grants NAG5-1 741 and NAGW-3938. A.S.E. also acknowledges funding from the ARCS Foundation. J.M. M. was supported by the Jet Propulsion Laboratory, California institute of Technology, under a contract with NASA. This research has made usc of the NASA/IPAC Extragalactic Databasc (NED) which is operated by the Jet l'repulsion Laboratory.

REFERENCES

Barvainis, R., Tacconi, I,., Antonucci, R., Alloin, D., & Coleman, 1'.1994, Nature, 371, 586

Briggs, F. 11., Sorar, E., & Taramopoulos, A. 1993, ApJ, 415, L99

Broadhurst, T. & Lehr, J. 1995, ApJ, submitted

Brown, R. L., & Vanden' out, 1'. A. 1991, AJ, 102, 1956

Brown, R. L., & Vanden Bout, P. A. 1992, ApJ, 397, L19

Chambers, K. C. & Charlot, S. 1990, ApJ, 348, L1

Chambers, K. C., Miley, G. K., & Joyce, R. R. 1988, ApJ, 329, L75

Chambers, K. C., Miley, G. K., & van Breugel, W. J. M. 1987, Nature, 329, 604

Chambers, K. C., Miley, G. K., & van Breugel, W. J. M. 1988, ApJ, 327, 1,47

Chambers, K. C., Miley, G. K., & van Breugel, W. J. M. 1990, ApJ, 363, 21

Chini, R., & Krügel, E. 1994, A&A, 288, L33

Dey, A., Spinrad, H., & Dickinson, M. 1995, ApJ, 440, 515

Djorgovski, S., Spinrad, 11., Pedelty, J., Rudnick, L., & Stockton, A. 1987, AJ, 93, 1307

Dunlop, J. S. Hughes, D. H., Rawlings, S., Eales, S., & Ward, M. J. 1994, Nature, 370, 347

Dunlop, J. S., & Peacock, J. A. 1993, MNRAS, 263, 936

Eales, S. A. & Rawlings, S. 1993, ApJ, 411, 67

Eales, S. A. & Rawlings, S. 1995, ApJ, submitted

Eales, S. A., Rawlings, S., Dickinson, M. Spinrad, H., Hill, G. L., & Lacy, M. 1993, ApJ, 409, 578

Eisenhardt, P. & Dickinson, M. 1992, ApJ, 399, L47

Elston, R., McCarthy, P. J., Eisenhardt, P., Dickinson, M., Spinrad, 11., Januzzi, B. T., & Mahoney, P. 1994, AJ, 107, 910

Evans, A. S. & Sanders, D. B. 1995, in preparation

Golombek, D., Miley, G. K., & Neugebauer, G. 1988 AJ, 95, 26

Graham, J. R. & Liu, M. C. 1995, ApJ, in press

Graham et al. 1994, ApJ, 420, L5

Guelin, M., Kramer, C., & Wild, W. 1995, IRAM Newsletter, 19, 17

Gusten, R., Serabyn, E., Kasemann, C., Schinckel, A., Schneider, G ., Schulz, A., & Young, K. 1993, ApJ, 402, 537

Heckman, T. M., Smith, E. P., Baum, S. A., van Breugel, W. J. M., Miley, G . K., Illingworth, G. D., Bothun, G. D., & Balick, B. 1986, ApJ, 311, 526

Helou, G., Khan, I. R., Malek, I,., & Boehmer, L. 1988, ApJS, 68, 151

Lilly, S. 1988, ApJ, 333, 161

Lilly, S. & Longair, M. 1984, MNRAS, 211, 833

Matthews, H. E. 1992, in The James Clerk Maxwell Telescope: A Guide for the Prospective User

Mozzarella, J. M., Graham, J. R., Sanders, D. B. &, 1 Djorgovski, S. 1993, ApJ, 409, 170

McCarthy, 1'. J. 1988, Ph.D. Thesis, U.C. Berkeley

McCarthy, P. J. 1993, ARA&A, 31, 639

McCarthy, P. J., Elston, R., & Eisenhardt, P. 1992, A pJ, 387, 1,29

McCarthy, P. J., van Breugel, W. J. M., Spinrad, H., & Djorgovski, S. 1987, ApJ, 321, 1,29

Miley, G. K. 1992, in Science with the Hubble Space Telescope: proceedings ST_ECF STSCI Workshop, eds P. Benvenuti and E. Schreier (European Southern Observatory,

Garching bei Menchen), 1

Mirabel, I. F. 1989, ApJ, 340, 1,13

Mirabel, 1. F., Sanders, D. 13., & Kazès 1989, ApJ, 340, L9

Rigler, M. A., Lilly, S. J., Stockton, A., Hammer, F., & Le Fèvre, O. 1992, ApJ, 385, 61

Röttgering, 11.1993, PhD Thesis, Rijksuniversiteit te Leiden, The Netherlands

Röttgering, H., Miley, G. K., Jennes, 1'., Sleath, J., van Ojik, R., & van der Werf, P. 1995, The JCMT Newsletter, 4, 32

Rowan-Robinson, M., et al. 1993, MNRAS, 261, 513

Sanders, D. B., Scoville, N. Z., & Soifer, B. T. 1991, ApJ, 370, 158

Sanders, D. B., Scoville, N. Z., Tilanus, R. P. J., Wang, Z., & Zhou, S. 1993, in Back to the Galaxy, eds S. Holt and F. Verter (New York: AIP), 311

Sanders, D. B., Soifer, B. T., Elias, J. H., Neugebauer, G., & Matthews, K. 1988, ApJ, 328, 1,35

Scoville, N. Z., & Sanders, D. B. 1987, in interstellar Processes, eds D. Hollenbach and H. Thronson (Dordrecht: Reidel), 21

Serjeant, S., Lacy, M., Rawlings, S., King, L. J., & Clements, D. L. 1995, MNRAS, in press

Soifer, 11. T., Cohen, J. G., Armus, I,., Matthews, K., Neugebauer, G., & Oke, J. B. 1995, ApJ, 443, L65

Solomon, P. M., Downes, D., & Radford, S. J. E. 1992a, ApJ, 398, 1,29

Solomon, P. M., Radford, S. J. E., & Dowries, D. 1992b, Nature, 356, 318

Spinrad, H., & Djorgovski, S. G. 1984a, ApJ, 280, L9

Spinrad, H., & Djorgovski, S. G. 1984b, ApJ, 285, L49

Telesco, C. M. 1993, MNRAS, 263, L37

Trentham, N. 1995, MNRAS, in press

Tsuboi, M., & Nakai, N. 1992, PASJ, 44, L241

Uson, J. M., Bagri, D. A., & Cornwell, T. J. 1991, Phys. Rev. Lett., 67 , 3328

Windhorst, R., et al. 1991, ApJ, 380, 362

This manuscript was prepared with the A AS LaTeX macros v3.2Beta.

Figure Captions

Figure 1. NRAO 12m spectra of 8 HzPRGs ranging from redshift 1 to 4. The intensity scale is main beam brightness temperature. A linear baseline has been subtracted from each spectrum. Vertical dashed lines mark velocities corresponding to the redshift of the indicated emission lines observed for that galaxy. Otherwise, the zero velocity corresponds to the average redshift of emission lines observed for that galaxy. Note the "features" in the CO(4 → 3) spectrum of B2 0902+34 (at ∼ +200 km s^{-1}) and the CO(3 → 2) spectrum of 4C 28.58 (at ∼ -300 km s-l).

Figure 2. IRAM 30m and JCMT 15m spectra of 4C 23.56 (z = 2.479) and 4C 28.58 (z = 2.951). The intensity scale is main beam brightness temperature. A linear baseline has been subtracted from each spectrum. Vertical dashed lines mark velocities corresponding to the redshift of the indicated emission lines observed for 4C 23.56. For the 4C 28.58 spectra, the zero velocity corresponds to the average redshift of emission lines observed for the galaxy. Note that the "features" in the 15m CO(7 → 6) spectrum of 4C 23.56 and the 12m CO(3 → 2) spectrum of 4C 28.58 are not present in the 30m spectra of these galaxies.

Figure 3. IRAM 30m spectra of 3C 368 (z = 1.132). The intensity scale is main beam brightness temperature. A linear baseline has been subtracted from each spectrum. The zero velocity corresponds to the average redshift of emission lines observed for 3C 368.

Figure 4. IRAM 30m spectra of 4C 41.17 (z = 3.797) and B2 0902+34 (z = 3.397). The intensity scale is main beam brightness temperature. A linear baseline has been subtracted from each spectrum. Vertical dashed lines mark velocities corresponding to the redshift of the indicated emission lines observed for that galaxy. Note that the 'feature' in the 12m CO(4 → 3) spectrum of B2 0902+34 is not present in the 30m spectrum.

Figure 5. IRAM 30m spectra of TX 0200+015 and MG 1019-}054. The intensity scale

is main beam brightness temperature. A linear baseline has been subtracted from each spectrum. The zero velocity corresponds to the average redshift of emission lines observed for that galaxy.

Figure 6. Plot of CO luminosity and H_2 mass vs. redshift for the 11 HzPRGs discussed in this paper, in addition to F102I4+4724, the Cloverleaf Quasar (H1413+135), the Milky Way, and several low-redshift ULIGs and JRAS-selected powerful radio galaxies ($q_o = 0.5$, $H_0 = 100\ h$ km s^{-1} Mpc^{-1}, $\alpha = 4\ M_\odot$ (K km s^{-1} $pc^2)^{-1}$). The upper limit molecular gas masses determined for 3C 368, 4C 23.56, B2 0902+34, and 4C 41.17 indicate that these galaxies have molecular gas masses comparable to or Icss than IR 14348-1447 and 4C 12.50. Note there is evidence that the apparently high Lee, (and thus $M(H_2)$) of F 10214+4724 and H1413+135 is due to lensing.

Figure 7. Rest-frame SEDs for 8 HzPRGs, the LzPRG 4C 12,50, and the hyperluminous infrared galaxy F10214+4724 (*g.* = 0.5, $H_0 = 100\ h$ km s^{-1} Mpc^{-1}). The dashed lines represent smooth fits to F 10214 +4724 and 4 C 12.50 data. Panels (l-3) HzPRGs observed in CO (this paper). Panels (4-8) Five additional HzPRGs with published optical- to-UV and radio photometry. References for data: For F10214 +4 724 - all data are from Rowan - Robinson et al. (1 993), except for the more recent 20μm measurement from Telesco (1993). For the radio galaxies - IRAS upper limits were determined by us from ADDSCAN/SCANPI processing (Helou et al. 1988) of the data in all four IRAS bands (12, 25, 60, 100 pm); the submillimeter data are from Chini & Krügel (1994), Dunlop et al. (1 994), and Eales et al. (1993); the radio data are from NED, except for 4C 41.17 (Dunlop et al. 1994); the near-ir/optical data are from Chambers & Chariot (1990) for 3C 368, from Chambers et al. (1988) for 4C 40.36, from Windhorst et al. (1991) for 53W002, from Eales & Rawlings (1993) for B3 0731 +438 and 3C 257, from Eales et al. (1993) for 6C 1232-I 39, from Lilly (1988) and Eisenhardt & Dickinson (1992) for B2 0902+34, and from Chambers et al. (1990) for 4C 41.17. Arrows indicate reported upper limits. Downward straight lines indicate continuum

level after subtraction of estimated contribution from optical emission line(s) (e.g. Eisenhardt & Dickinson 1992; Eales & Rawlings 1993; Graham et al. 1994).

TABLE 1

JOURNAL OF OBSERVATIONS

Source	coord. 1950 α			coord. 1950 δ			z	CO line	Site	Date m/y	time hr	T_{sys} K
TX 0200+015	02	00	08.20	01	34	45.95	2.230	3 → 2	30m	12/94	1.2	195
3C 68.2	02	31	24.82	31	21	11.2	1.575	2 → 1	12111	12/92	9.3	235
4C 41.17	00	47	20.79	41	34	04.5	3.797	4 → 3	12m	12/92	7.9	185
										05/94	17.5	170
										10/94	20.8	200
								4 → 3	30m	10/94	29.2	250
								6 → 5	30111	10/94	29.2	370
								9 → 8	30m	10/94	29.2	510
TX 0828+-193	08	28	01.22	19	23	23.8	2.572	3 → 2	12rll	06/93	16.9	190
132 0902+34	09	02	24.77	34	19	57.8	3.397	4 → 3	12r()	10/93	23.4	225
										05/94	29.2	170
								4 → 3	30m	08/94	8.9	220
										12/94	7.8	190
								5 → 4	3011)	06/94	10.0	270
										08/94	9.7	400
										12/94	7.8	210
								8 → 7	30m	12 /94	7.8	320
MG 1019+054	10	16	56.82	05	49	39.3	2.765	3 → 2	30m	12/94	1.2	210
4C 26.38	12	29	54.32	26	20	40.0	2.609	3 → 2	12111	06/93	9.4	180
3C 368	18	02	45.60	11	01	13.8	1.132	2 → 1	12m	10/93	31.1	250
										05/94	9.9	190
								2 → 1	30m	06/94	7.7	290
										12/94	2.3	220
4C 23.56	21	05	00.96	23	19	37.7	2.479	3 → 2	30m	12/94	7.7	215
								4 → 3	30m	12/94	7.7	310
								7 → 6	15rll	10/93	11.0	330
										04/94	4.6	335
										09/94	5.2	480
MG 2141+19	21	41	46.97	19	15	25.9	3.594	4 → 3	12111	10/94	14.4	190
										01 /95	3.1	200
4C 28.58	23	49	26.89	28	53	47.88	2.951	3 → 2	12111	06/93	22.0	200
										05/94	18.2	185
								3 - + 2	30m	08/94	5.4	170
								8 - + 7	15111	10/93	8.9	400

REFERENCES.— Positions and Redshifts: (1) TX 0200+ 015- Röttgering 1993; Evans& Sanders 1995; (2) 3C 68.2- McCarthy 1988; (3) 4C 41.17- Chambers, Miley, & van Breugel 1990; Wale. & Rawlings 1993; (4) TX 0828+193 - Röttgering 1993; (5) 132 0902+34 - Lilly 1988; Uson et al. 1991; Eales & Rawlings 1993; (6) MG 1019+054 - Dey et al. 1995; (7) 4C 26.38- K. Chambers, private communication; (8) 3C 368- e.g. Djorgovskiet al. 1987; (9) 4C 23.56- K. Chambers, private communication; Evans & Sanders 1995; (1 O) MG 2141 +19 - Eales & Rawlings)995; (11) 4C 28.58- Miley 1992; K. Chambers, private communication.

TABLE 2

CO EMISSION LINE DATA

Source	Site	CO line	$\nu_{v=0}$ (GHz)	v_{offset} (km s^{-1})	Δv_{res} (km s^{-1})	T_{rms}[a] (mK)	$S_{CO}\Delta v$ (Jy km s^{-1})	L'_{CO}[b] ($\times 10^9 h^{-2} L_\odot$)	$M(H_2)$[c] ($\times 10^{10} h^{-2} M_\odot$)
TX 0200+015	30m	3 → 2	106.99100	0	49	1.7	<2.7	<16	<6.5
3C 68.2	12m	2 → 1	89.52930	0	54	0.42	<3.7	<28	<11
4C 41.17	12nl	4 → 3	96,11024	0	56	0.093	<0.83	<6.2	<2.5
	30m	4 → 3	96.11024	0	50	0.79	<1.2	<9.5	<3.8
				1100	50	0.64	<1.0	<7.8	<3.1
				1750	50	1.4	<2.3	<18	<7.0
	30111	6 → 5	144.14699	0	50	1.0	<1.7	<0.58	...
				1100	50	1.1	<1.8	<0.61	...
				1750	50	2.2	<3.6	<1.2	...
	30m	9 → 8	216.15852	0	36	1.8	<2.4	<0,36	...
				1100	36	1.8	<2.3	<0.35	...
				1750	37	8.0	<1o	<1.5	...
TX 0828+193	12m	3 → 2	96.80739	0	50	0.26	<2.2	<17	<6.7
B2 0902+34	12m	4 → 3	104.85820	200	51	0.26	<2.2	<14	<5.7
				-300	51	0.15	<1.3	<8.5	<3.4
	30m	4 → 3	104.85820	200	46	0.46	<0.70	<4.5	<1.8
		5 4 4	131.06530	200	37	0.40	<0.56	<2.3	...
		8 → 7	209.65240	200	38	1.8	<2.4	<0.39	
MG 1019+054	30m	3 → 2	91.84500	0	49	1.4	<2.2	<18	<7.4
4C 26.38	12m	3 → 2	95.81490	0	50	0.45	<3.8	<30	<12
3C 368	12111	2 → 1	108.13220	100	50	0.33	<2.8	<13	<5.1
				-400	50	0.23	<1.9	<8.8	<3.5
	30m	2 → 1	108.13220	100	50	1.3	<2.0	<9.0	<3.6
				-500	50	0.86	<1.4	<6.2	<2.5
	30m	3 → 2	162.19300	0	50	1.8	<2.9	<5.8	<2.3
	30m	4 → 3	216.24800	0	42	2.5	<3.5	<4.0	<1.6
4C 23.56	30111	3 → 2	99.39520	0	48	0.68	<1.0	<7.5	<3.0
		4 → 3	132.52100	0	47	1.0	<1.6	<6.8	<2.7
	15m	7 → 6	231,86311	0	39	0.86	<4.0	<0.52	
MG 2141+19	12111	4 4 3	100.35716	0	54	0.24	<2.0	<14	<5.7
4C 28.58	12m	3 → 2	87.52113	0	48	0.23	<1.8	<17	<6.9
	30m	3 → 2	87.52113	0	43	0.80	<1.2	<11	<4.5
	15nl	8 → 7	233.54438	0	39	1.6	<7.1	<0.93	..

[a] Therms temperatures are given in terms of main beam brightness temperature c.
[b] Assuming $gO = 0.5$, $H_0 = 100\ h$ km S^{-m} Mix^{1}.
[c] Assuming $\alpha = 4\ M_\odot$ (K km s^{-1} pc^2)$^{-1}$ (see text).

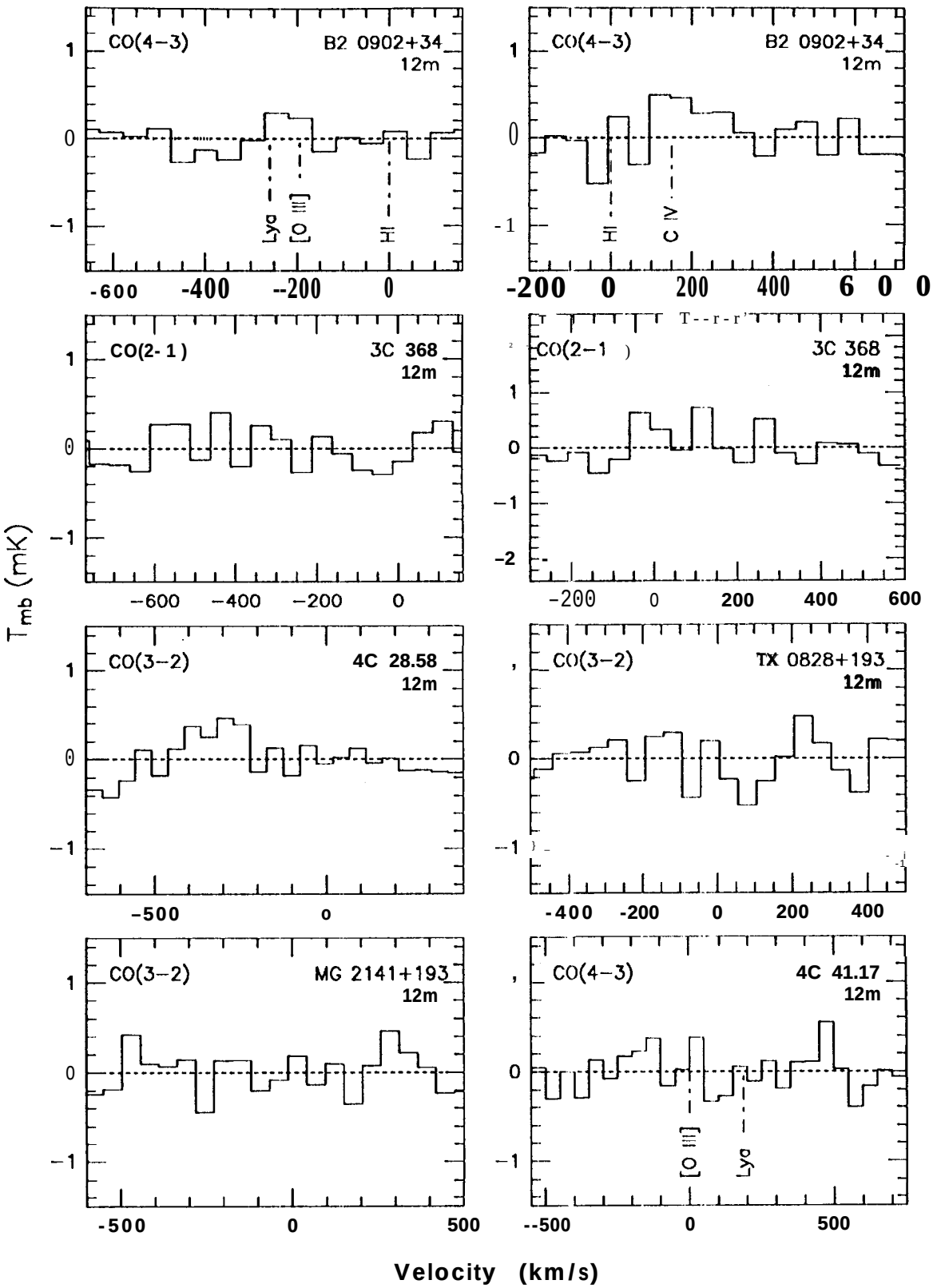
CO(4−3)
B2 0902+34
12m
Lyα
[O III]
HI
CO(4−3)
B2 0902+34
12m
HI
C IV
CO(2-1)
3C 368
12m
CO(2−1)
3C 368
12m
CO(3−2)
4C 28.58
12m
CO(3−2)
TX 0828+193
12m
CO(3−2)
MG 2141+193
12m
CO(4−3)
4C 41.17
12m
[O III]
Lyα
T_{mb} (mK)
Velocity (km/s)

Fig. 1.

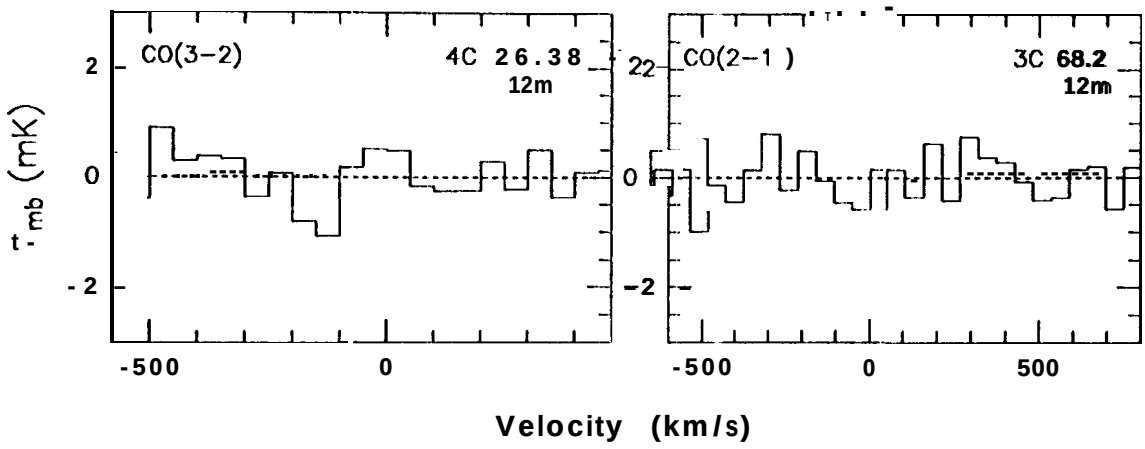
CO(3-2)
4C 26.38
12m
CO(2-1)
3C 68.2
12m
2
0
-2
22
0
-2
-500
0
-500
0
500
T_{mb} (mK)
Velocity (km/s)

Fig. *1*.-

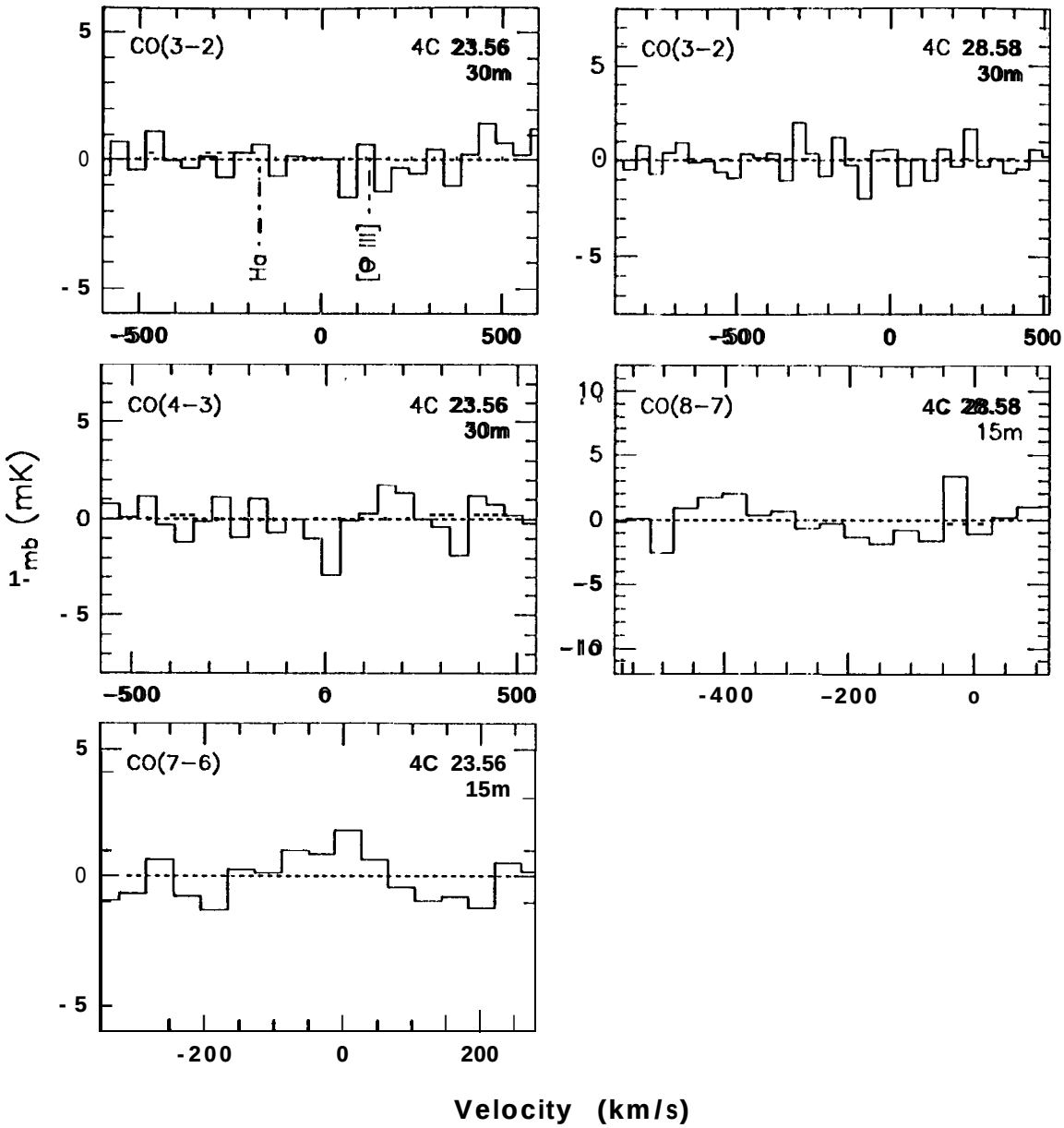
CO(3-2)
4C 23.56
30m
Hα
[OIII]
CO(3-2)
4C 28.58
30m
CO(4-3)
4C 23.56
30m
CO(8-7)
4C 28.58
15m
CO(7-6)
4C 23.56
15m
1 mb (mK)
Velocity (km/s)

Fig. 2.

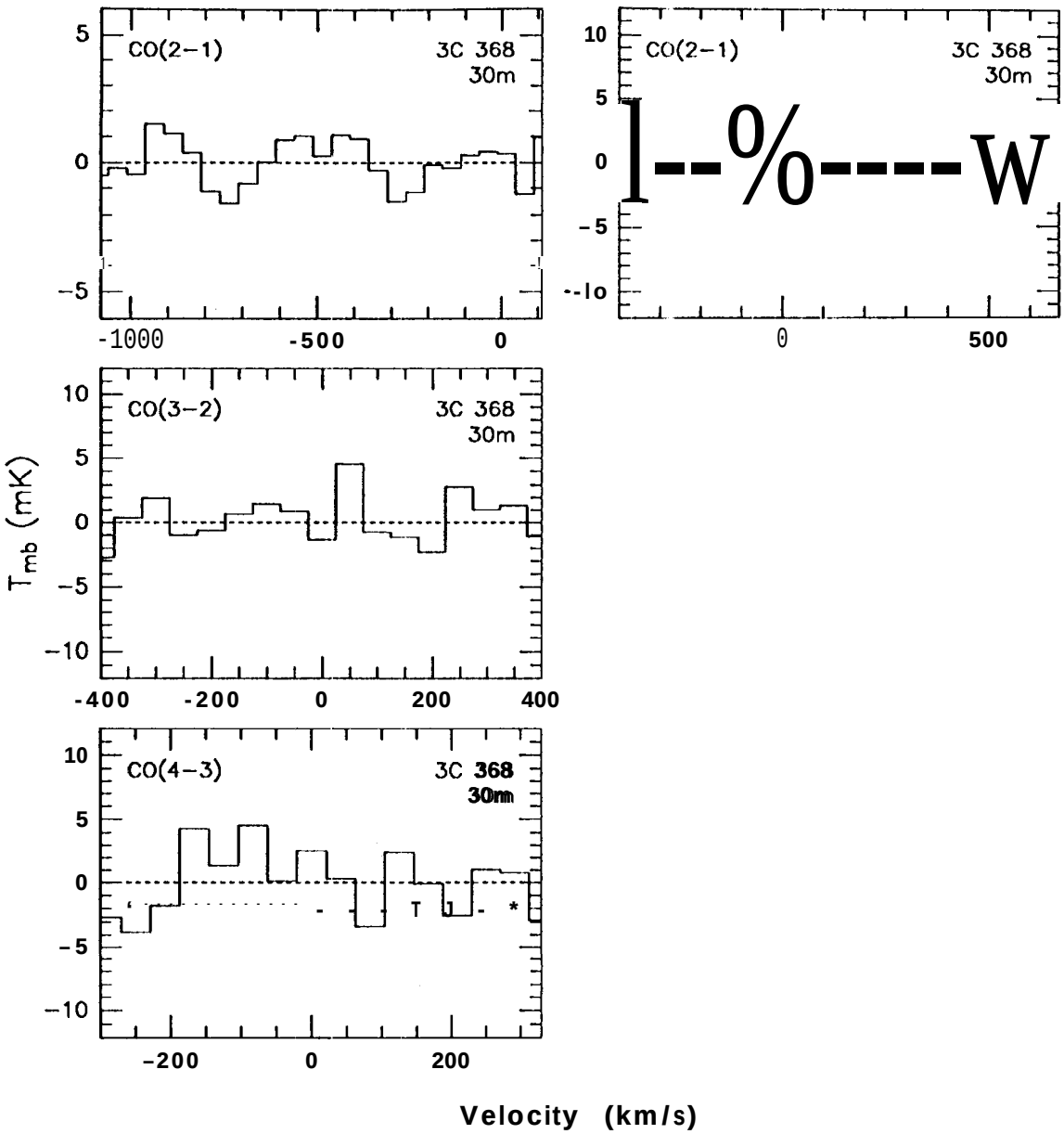
CO(2−1)
3C 368
30m
CO(2−1)
3C 368
30m
CO(3−2)
3C 368
30m
CO(4−3)
3C 368
30m
T_{mb} (mK)
Velocity (km/s)

, Fig. 3.-

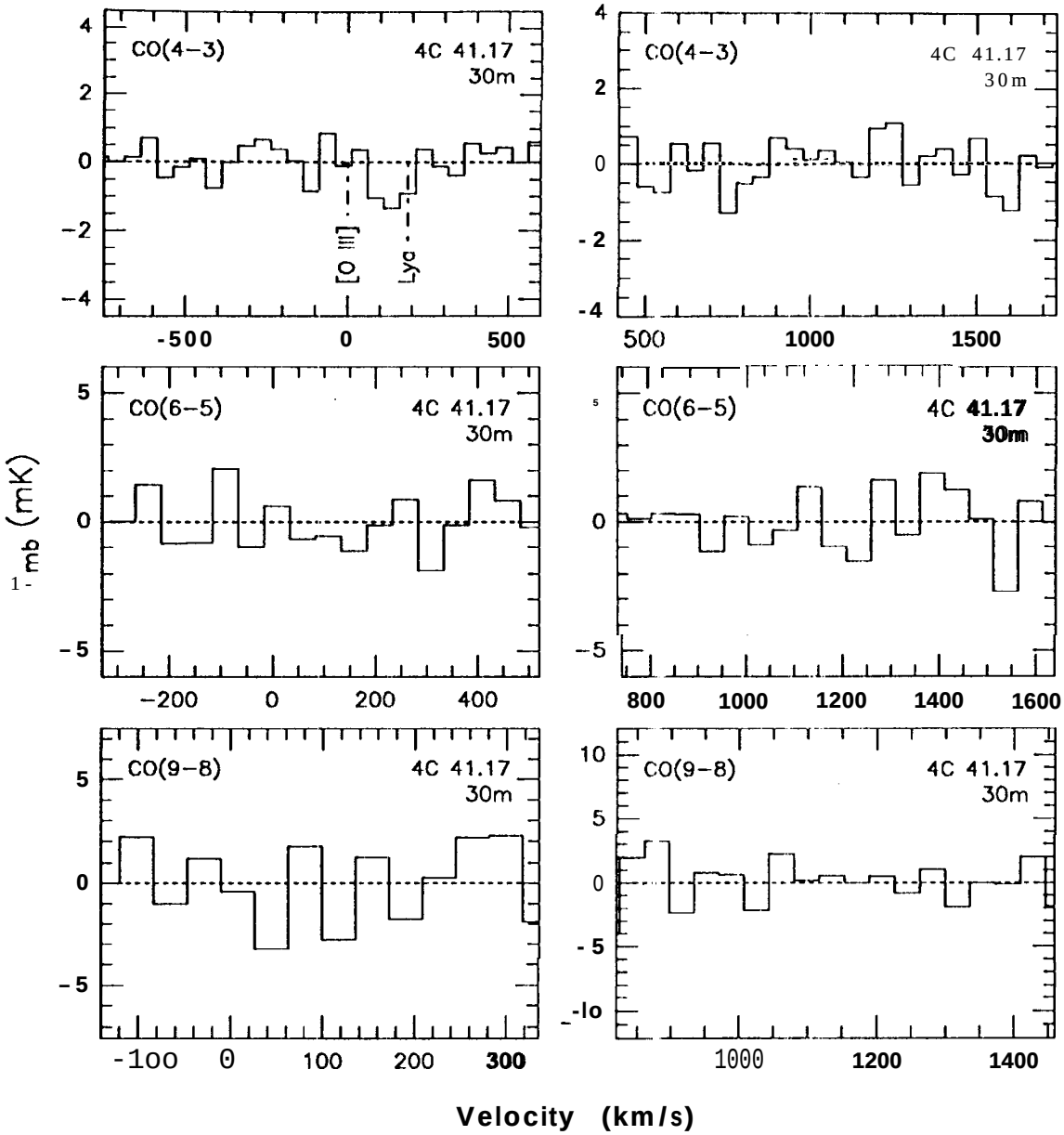

Fig. 4.-

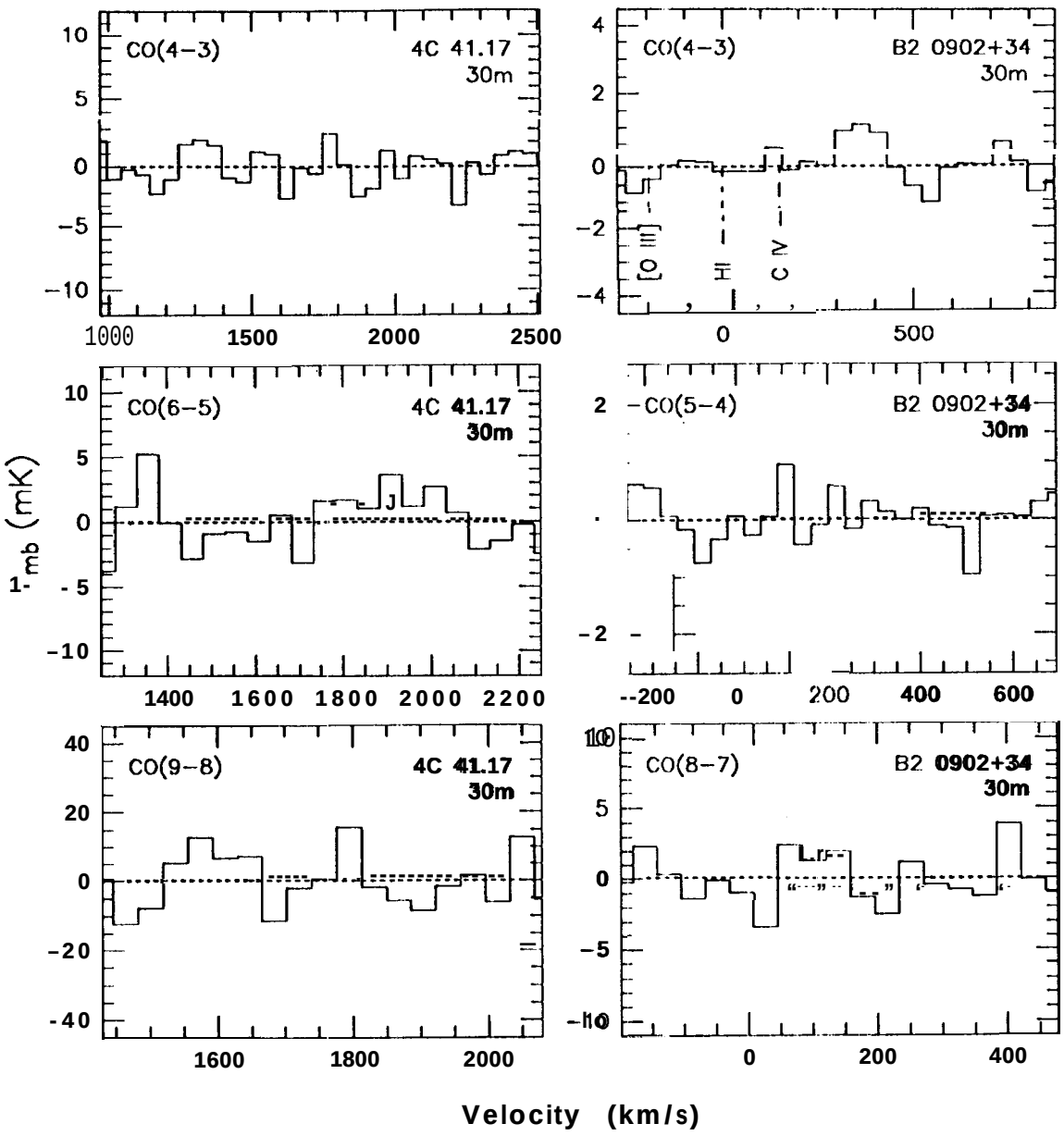
CO(4−3)
4C 41.17
30m
CO(4−3)
B2 0902+34
30m
[O III]
Hβ
C IV
CO(6−5)
4C 41.17
30m
CO(5−4)
B2 0902+34
30m
CO(9−8)
4C 41.17
30m
CO(8−7)
B2 0902+34
30m
T_{mb} (mK)
Velocity (km/s)

Fig. 4.-

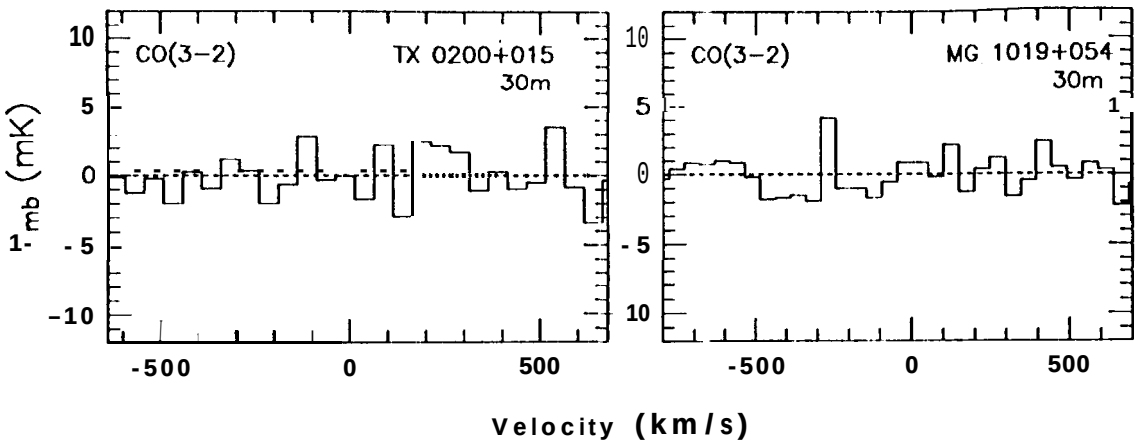
CO(3–2)
TX 0200+015
30m
CO(3–2)
MG 1019+054
30m
10
5
0
-5
-10
-500
0
500
T_{mb} (mK)
Velocity (km/s)

Fig. 5.

Fig. 6.

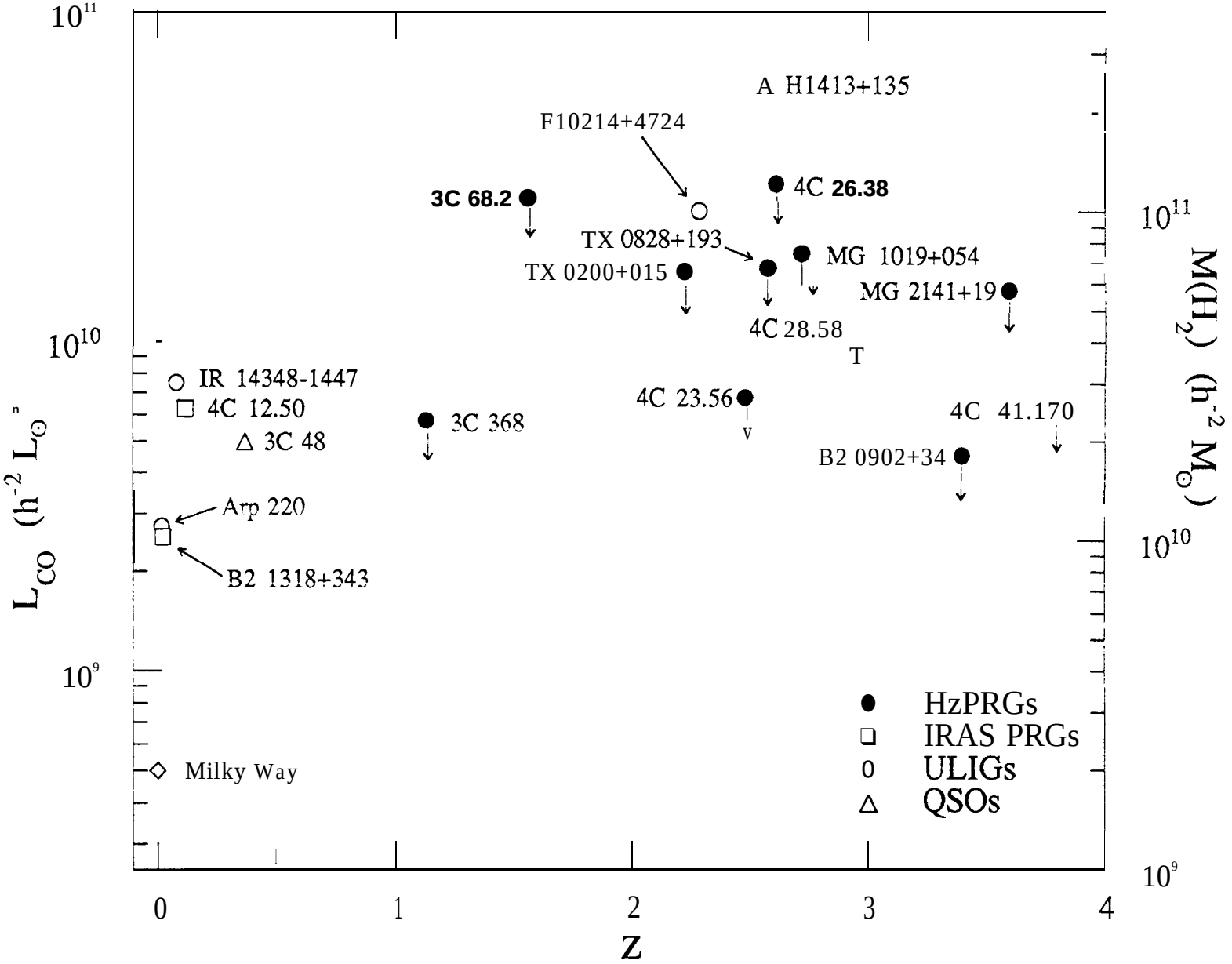
A H1413+135
F10214+4724
3C 68.2
4C 26.38
TX 0828+193
MG 1019+054
TX 0200+015
MG 2141+19
4C 28.58
T
IR 14348-1447
4C 12.50
3C 48
3C 368
4C 23.56
V
4C 41.170
B2 0902+34
Arp 220
B2 1318+343
Milky Way
HzPRGs
IRAS PRGs
ULIGs
QSOs
10^{11}
10^{10}
10^{9}
L_{CO} (h^{-2} $L_{\odot}$)
$M(H_2)$ (h^{-2} $M_{\odot}$)
0
1
2
3
4
Z

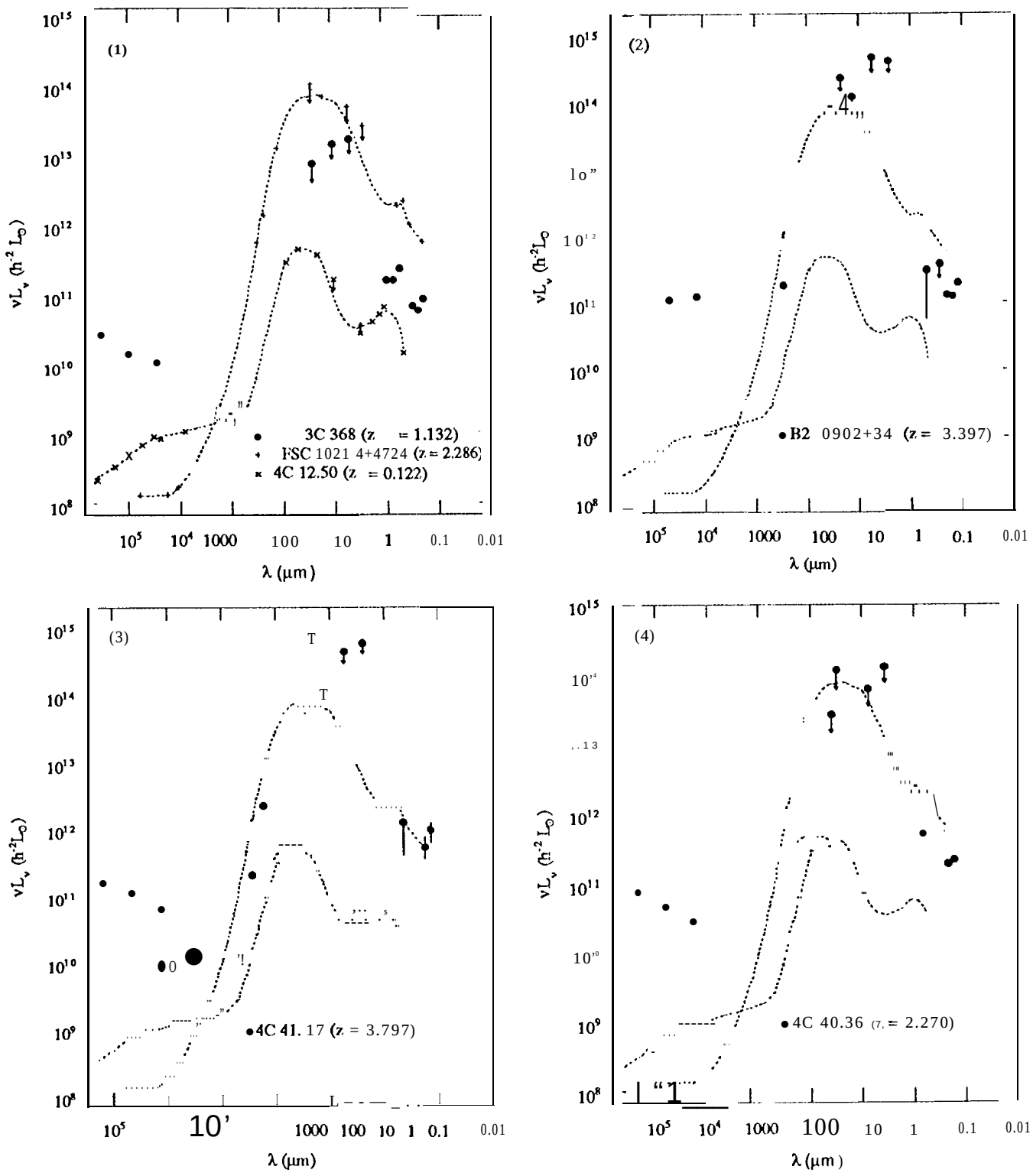
(1)
3C 368 (z = 1.132)
FSC 1021 4+4724 (z = 2.286)
4C 12.50 (z = 0.122)
λ (μm)
(2)
B2 0902+34 (z = 3.397)
λ (μm)
(3)
4C 41.17 (z = 3.797)
λ (μm)
(4)
4C 40.36 (z = 2.270)
λ (μm)

Fig. 7.-

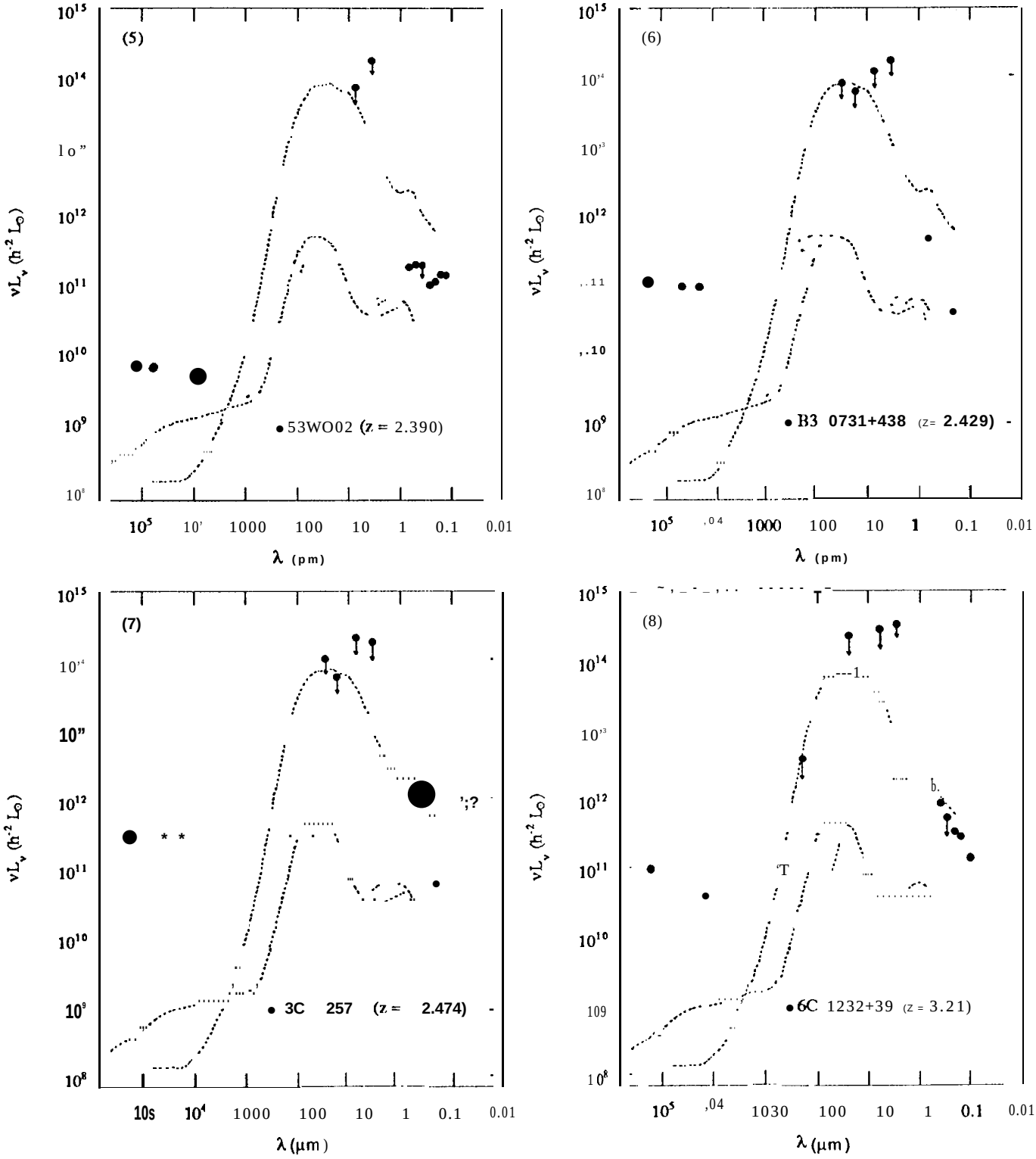
(5)
(6)
(7)
(8)
53WO02 (z = 2.390)
B3 0731+438 (z= 2.429)
3C 257 (z = 2.474)
6C 1232+39 (z = 3.21)
νL_ν (h^-2 L_⊙)
λ (pm)
λ (μm)

Fig. 7.